Mechanical Vibration Analysis of Induction Machine Based on MEMS Sensor

Mechanical Vibration Analysis of Induction Machine Based on MEMS Sensor

Jun Chen, Jia Wang and Tao Zhou

Luoyang Normal University, Physics and Electronic Information Department, 471934 Luoyang, China

Abstract. Induction motors are widely used in industrial production, and the consequent motor vibration hazards cannot be ignored. In this paper, a micro-vibration measuring equipment based on MEMS technology is designed for the measurement of motor vibration. The application circuit based on ADXL 203 micro accelerometer is designed. The device parameters of the circuit are analyzed in detail. The hardware circuit of the sensor is adjusted, and the stainless steel enclosure of the sensor is designed. The sensor can be conveniently attached to the surface of the motor under test. The measuring software is designed. The initialization settings of microprocessor and sensor are described in detail. The vibration frequency and motor speed are measured on the test table. Experimental results demonstrate the practicability of the system.

1. Introduction

The existing motor vibration parameter measurement technology mainly has several aspects: current spectrum analysis method, mechanical vibration signal analysis method, optical fiber method, etc. The idea of these methods is the same: to obtain the vibration-related data through different detection methods, and then extract the signal with fault characteristics from the data through the algorithm. The current spectrum analysis method [1] is to analyze the current spectrum diagram of the motor stator by adding a current sensor on the phase line of the motor stator and obtain the cause of the fault [2]. The spectral kurtosis and envelope analysis in [3] and the stray flux measurement in [4] are used to measure the motor vibration. Mechanical vibration signal analysis method is to directly collect vibration signals of motor through vibration sensor, and then use frequency spectrum [5], transient power spectrum [6], dual-order spectrum, wavelet analysis and other methods to obtain vibration parameters.

With the rapid development of MEMS (Micro Electro Mechanical System) technology, it is entirely possible to integrate high precession sensitive elements, analog-digital conversion parts, microprocessor, and high order filter and communication interfaces circuit into the micro sensor. In this article, the high precession digital micro accelerometer based on MEMS is used as the measure sensor, the implementation, calibration, characterization and testing are presented. This kind of accelerometers have been proved to be one of the most promising sensors for smart instruments.

2. Hardware of the accelerometer

Compared with many other MEMS accelerometer with the similar properties, the accelerometer FXLS8471Q is chosen. Owning to integrating the comb type differential capacitors and poly-silicon surface micro-machined structure built on top of a silicon wafer, the accelerometer is endowed with the characteristics of high sensitivity and perfect temperature stability. Also the small volume, low power

consumption, multifunction and digital signal output are the advantages. So it is especially suitable for the long time acceleration measurement. It has dynamically selectable acceleration full-scale ranges of $\pm 2g/\pm 4g/\pm 8g$. The 14 bit ADC resolution can reach $0.244mg/LSB$. The IIC serial digital interface is provided to communicate with the MCU at the mode 100 kHz and fast mode 400 kHz.

In order to realize the stability of the circuit and remove the high frequency noise from the power supply, the internal and external power pins are connected to ground through $0.1\mu F$ ceramic capacitors. The SCL and SDA pins are connected to pull-up resistors to ensure the high and low signal change effectively. SA0 and SA1 pins are connected to the ground to set the address 0x1E which used to be recognized by MCU. The circuit schematic is in Fig.1 and final PCB board is in Fig.2.

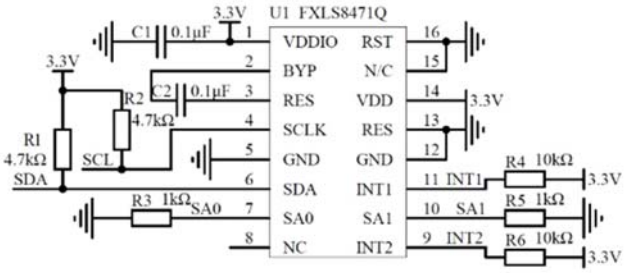

Figure 1. Schematic diagram

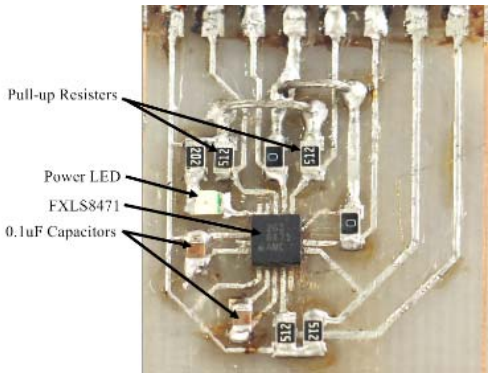

Figure 2. Circuit PCB board

Figure 3. Sensor shell and inner circuit

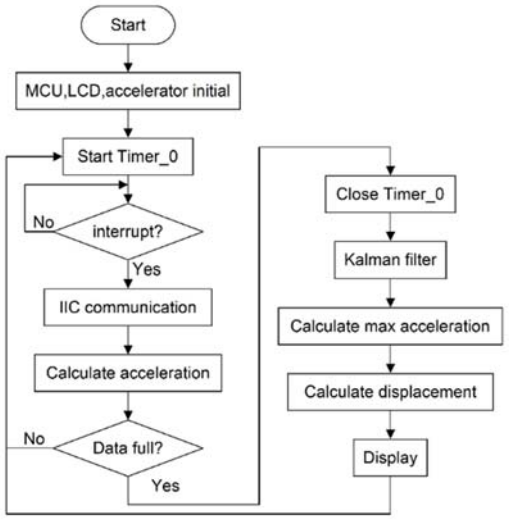

Figure 4. Flow diagram

The circuit board of the sensor is packaged in the cylinder stainless steel shell which bottom diameter is 29cm and height is 29cm. They are shown in the Fig.3. Compared with the, the sensor has its advantages in volume. With the stainless steel shell, the electromagnetic interference can be shielded. The bottom of the shell is sealed by the NdFeB magnet steel disc with the epoxy resin. So that the shell can be adsorbed anywhere on the mental surface of the motor tightly and would not change the position.

3. Software Design

The software is constructed by four initializations, one interrupt, one communication, and three algorithms. At the beginning of the software, the MCU, LCD, accelerometer, Timer_0 are initialized. In

the interrupt of Timer_0, the IIC communication is executed. The calculation of Kalman filter, accelerometer and displacement are finished in the main function. The flow chart is in Fig.4.

4. System Initialization

4.1. Main Clock Initialization

The UCS (Unified Clock System) module in the MSP430F6638 supports low system cost and ultralow power consumption. Using the internal clock signals, the user can select the best balance of performance and low power consumption.

The displacement algorithm and Kalman filter algorithm need high frequency clock to be processed. So the 32.768 kHz REFOCLK (Reference out clock) is used as the source of main clock. Between the REFOCLK and the main clock, the FLL (Frequency lock loop) unit was added. The DCO (Digitally controlled oscillator) in the FLL is used to increase the main clock frequency. The output clock frequency DCOCLK is calculated by (1).

$$f_{\mathrm{DCO}} = (N+1) f_{\mathrm{FLLREFCLK}} \tag{1}$$

Which $f_{\mathrm{FLLREFCLK}}$ is $32.768\mathrm{kHz}$. The main clock frequency f_{DCO} is designed to 25MHz, so the $N = 762$.

4.2. Timer_0 initialization

The Timer_0 is used to control the sample period precisely. In the Timer_0 interrupt routine, the IIC program is called to acquire the data from the sensor. The sample period is controlled by the overflow counter register. The counter is set at the up-mode. After the overflow, the register TA1CCR0 is cleared automatically. The interrupt frequency $f_{\mathrm{interrupt}}$ is set to 1250Hz. Different from the main clock, the clock source of the Timer is SMCLK, which is good for the noise proof and decrease the power consumption. The SMCLK frequency f_{SMCLK} is $10\mathrm{kHz}$, which use the VLOCLK as the clock source. The upper limit of the counter TA1CCR0 is calculated in (2), and the TA1CCR0=7.

$$\mathrm{TA1CCR0} = \frac{f_{\mathrm{SMCLK}}}{f_{\mathrm{interrupt}}} - 1 \tag{2}$$

4.3. Accelerometer Register set

The working mode of FXLS8471Q are defined by the relevant registers. According to the design requirements, two registers with addresses 0x2A and 0x2B are needed to be set.

The modes in 0x2A are as follows: the auto-wake sample frequency when the device is in sleep mode, ODR selection, reduced noise mode, normal or fast read, and standby active. With the design requirements, the sensor is required working at non-sleep mode, the ODR is 800Hz, low-noise mode, normal read mode. As a result, the register is set as 0x11.

The modes in 0x2B are: self-test enable, software reset, auto-sleep mode enable, and oversampling ratio selection. With the design requirements, the self-test, reset, and auto sleep modes are forbidden and high resolution mode is set. As a result, the register is set as 0x02.

After the MCU acquired the 14 bits data from the sensor, the data must be rebuilt. The sample data output registers store the current sample data. For example, the data register OUT_X_LSB store the low 8 bits of the X-axis data, the 2-7 bits are the data bits, 0-1 bits are the empty bits. The data register OUT_X_MSB store the high 8 bits of the data. So the binary code $Temp$ of the acceleration is calculated in (3).

$$Temp = (256 \cdot (OUT\_X\_LSB) + (OUT\_X\_MSB)) / 4 \tag{3}$$

4.4. Calculation of accelerometer value

From (3), the DC voltage bias is included in the acceleration result. The accelerometer contains a bias acceleration between $+1g \sim -1g$. While the vibration measure instrument is working, this bias will be added in the real vibration acceleration which can disturb the final displacement value, so it must be removed.

From the software, many vibration periods are collected in one Timer_0 interrupt. Among these periods, the max and min accelerations are picked out by the bubble sort algorithm and the average acceleration value is calculated by the max and min acceleration. This average acceleration value is the balance position of the displacement accumulation algorithm. The one quarter period which include the max value is picked out and after each value (sample point) of the period minuses the average acceleration value one by one, then the DC voltage bias between $+1g \sim -1g$ is removed and left the real acceleration value.

5. Experiment and data analysis

5.1. Test rig construction

The software on the host computer is developed by the LabVIEW from National Instrument. The data is acquired with the help of VISA (Virtual Instrument Software Architecture) drivers.

It is widely known that the way a sensor is mounted become a significant factor to compare results. Accelerometer is extremely sensitive to the position of mounting. The frequency and resonances are different at the same motor speed when the accelerometer is mounted at the different position. An effective position is adopted after large number of tests that the result is shown in the Fig.5.

With the help of couplers, the shafts of DM and DG are connected, also the torque is transmitted from the DM to DG, in another word, and the DG operates as the load of the DM. At the other side of the DG, the shafts of tachometer and DG are connected in the same way. The DM and DG used in this test are designed for the test rig specially.

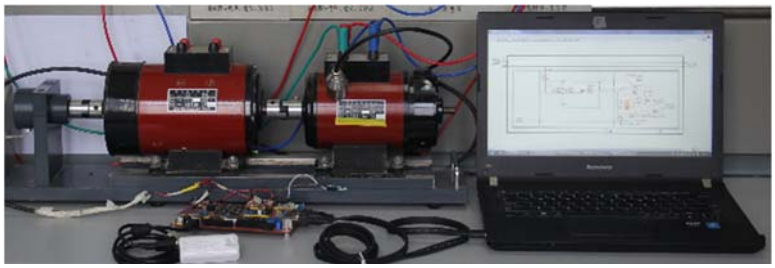

Figure 5. Test rig system

5.2. Vibration frequency experiments

The sensor is adsorbed on the left-top surface of the motor toughly so that the vibration of the motor can transmit to the sensor sufficiently. The rotate speed increases 125r/min each time from 1000r/min to 3000r/min and the data are acquired with each increase. These original data are transmitted to the host computer by serial port and the frequencies are figured out according to the frequency analysis. Take the speed 2800r/min for example, the original vibration waveform is in Fig.6. The waveform is a periodical sinusoidal wave with a lot of noise in agreement with the real condition.

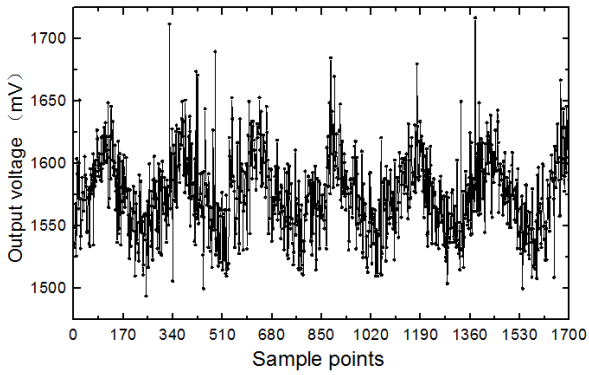

Figure 6. Original vibration waveform

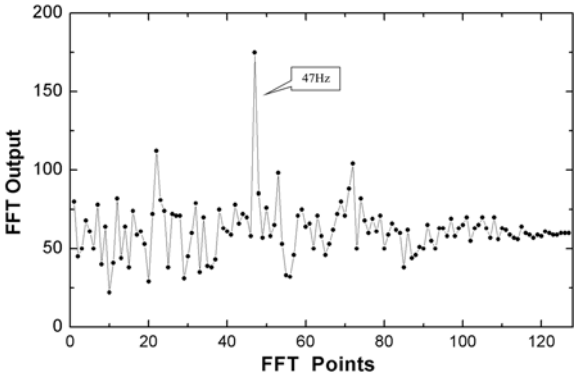

Figure 7. FFT result at 2800r/min

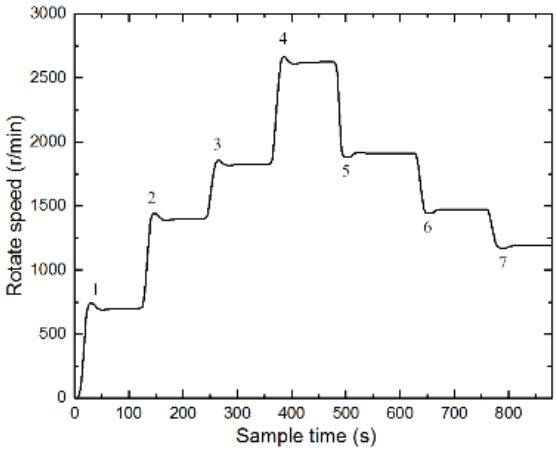

Figure 8. Speed continuous change test

After the data of the waveform are disposed by the Kalman filter and the noise data are removed, the effective data are sent to the host computer for the FFT. The result is in Fig.7 and the frequency of the motor is 47Hz, which is coincide with the speed 2800r/min .

Table 1 shows the vibration frequency test results from 1000r/min to 3000r/min with increment 125r/min . The sample frequency of the FFT is 128Hz and 512 points are sampled each time. Based on the precision features of the FFT, the resolution of the N points FFT calculation is F_S / N , F_S is the sample frequency. So the minimum frequency that can be distinguished by the FFT is 0.25Hz, so the step size of the calculation result is 0.25Hz.

Some errors exist between the real frequency and FFT frequency. The reason is that the quantization error and approximate calculation are unavoidable while the FFT is processing in the computer. When the error accumulate up to 0.25Hz, the error is return to zero such as the speed 1500r/min and 1875r/min .The errors have regularity within the range ± 0.1Hz . It indicates that the results are accurate. After the error compensation, the real vibration frequency is achieved.

5.3. Speed continuous change test

In order to test whether the instrument can trace the speed change continuously, the rotate speed of the motor is set as change 7 times from 0r/min to 2625r/min irregularly. The results of rotate speed is shown in Fig.8.

In the experiment, the motor driver is controlled by the signal from the host computer. After the signal comes, the motor reaches the control speed in a short time by the closed loop controller in the

motor driver. The instrument records every course immediately of the speed change. All the parameters of the course are in Table 1.

Table 1. Parameters of speed change

Serial number	Peak value (r/min)	Set speed (r/min)	Overshoot (σ)	Steady state error (r/min)
1	740	700	5.714%	0.47
2	1440	1400	5.714%	0.2
3	1857	1825	7.529%	0.3
4	2669	2625	3.667%	1
5	1883	1912	4.067%	0.8
6	1444	1470	5.882%	1
7	1169	1190	7.500%	0.65

6. Conclusion

The existing sensors of the MEMS technology are developing quickly. Many famous electronic company are focus on improving the ADC resolving ability and the multifunction of filters that can be programmed by the user aim to get satisfactory SNR. Accompanied by the rapid development of microprocessor, the processors are exhibiting high performance on the calculation of complex algorithm. With the progress of semiconductor technology, the voltage of the chip are lower and the extremely low power chip will be widespread used in the hand-held vibration measurement instruments. At last, the advanced algorithms of measurement data processing such as filter and data transformation will play the key role in the vibration measurement filed.

Acknowledgments

The authors wish to acknowledge the financial support of Science and technology key project in Henan province (Grant No.182102210430) and (Grant No.182102210435), Key Scientific Research Project of Higher Education in Henan province (Grant No.19A510018).

References

[1] R. R. Schoen et al., “Effects of time-varying loads on rotor fault detection in induction machines,” IEEE Trans. Ind. Applicat., vol. 31, pp.900–906, July/Aug. 1995.
[2] M. E. H. Benbouzid, “A review of induction motors signature analysis as a medium for faults detection,” IEEE Trans. Ind. Electron., vol. 47, no. 5, pp. 984–993, Oct. 2000.
[3] V. C. M. N. Leite et al., “Detection of localized bearing faults in induction machines by spectral kurtosis and envelope analysis of stator current,” IEEE Trans. Ind. Electron., vol. 62, no. 3, pp. 1855–1865, Mar. 2015.
[4] L. Frosini, C. Harlis¸ca, and L. Szabó, “Induction machine bearing fault detection by means of statistical processing of the stray flux measurement,” IEEE Trans. Ind. Electron., vol. 62, no. 3, pp. 1846–1854, Mar. 2015.
[5] S. J. Lacey, “An overview of bearing vibration analysis,” Maintenance Asset Manage., vol. 23, no. 6, pp. 32–42, Nov.Dec. 2008.
[6] R. Maier, “Protection of squirrel-cage induction motor utilizing instantaneous power and phase information,” IEEE Trans. Ind. Applicat., vol.28, pp. 376–380, Mar.Apr. 1992.